

# F and Fe co-doped TiO<sub>2</sub> with enhanced visible light photocatalytic activity

Yihe Zhang · Fengzhu Lv · Tao Wu ·  
Li Yu · Rui Zhang · Bo Shen · Xianghai Meng ·  
Zhengfang Ye · Paul K. Chu

Received: 31 October 2010 / Accepted: 17 March 2011 / Published online: 30 March 2011  
© Springer Science+Business Media, LLC 2011

**Abstract** Four different sols, pure TiO<sub>2</sub>, F doped TiO<sub>2</sub>, Fe doped TiO<sub>2</sub>, and F–Fe co-doped TiO<sub>2</sub> sols, were prepared by peroxidation at low temperature. The crystal structure, morphology, light adsorption, and photocatalytic properties of the pure and doped TiO<sub>2</sub> were examined by X-ray diffraction, transmission electron microscopy, and ultraviolet–visible spectrophotometry. The relationship between the average size, crystal type, range of visible light absorption, and photocatalytic activity and content and type of doped ions were investigated. The results showed that the average size of the F–Fe co-doped TiO<sub>2</sub> composed of both the anatase and rutile phases was the same as that of pure TiO<sub>2</sub>. Furthermore, the visible light photocatalytic activity of the F–Fe co-doped TiO<sub>2</sub> was significantly improved over pure TiO<sub>2</sub>, F-doped TiO<sub>2</sub>, and Fe-doped TiO<sub>2</sub> due to the large red shift in the light adsorption edge.

**Keywords** TiO<sub>2</sub> · Co-doping · Visible light · Photocatalytic property

---

Y. Zhang (✉) · F. Lv · T. Wu · L. Yu · R. Zhang · B. Shen ·  
X. Meng  
State Key Laboratory of Geological Processes and Mineral  
Resources, School of Materials Science and Technology, China  
University of Geosciences (Beijing), 100083 Beijing, People's  
Republic of China  
e-mail: zyh@cugb.edu.cn

Z. Ye  
Department of Environmental Engineering, Key Laboratory of  
Water and Sediment Sciences of the Ministry of Education,  
Peking University, 100871 Beijing, People's Republic of China

P. K. Chu  
Department of Physics and Materials Science, City University of  
Hong Kong, Tat Chee Avenue, Kowloon, Hong Kong, China

## 1 Introduction

Environmental pollution has aroused global concern and measures to mitigate related problems are extensively investigated. The phenomenon that irradiated TiO<sub>2</sub> electrode could decomposed water was first found by Fujishima [1]. Subsequently, the applications of TiO<sub>2</sub> to waste water treatment and air pollution control have been extensively investigated [2–4]. TiO<sub>2</sub> exhibits the strong redox ability that can convert pollutants into CO<sub>2</sub>, H<sub>2</sub>O, and other small molecules [5–7]. Studies on increasing the anatase content, which is the most active phase of TiO<sub>2</sub> in photocatalysis, have been performed. However, the low catalytic activity and difficulties associated with the efficient utilization of visible light and recycling have seriously hampered large-scale application of TiO<sub>2</sub> as a photocatalyst.

In order to improve the photocatalytic activity under visible light, TiO<sub>2</sub> nanoparticles are doped with various elements. The band gap which is responsible for the photo-response can be narrowed by doping with nonmetals such as N, C, F, S, etc. [8–11]. The separation of photo excited electrons and holes which play important roles in the photocatalytic activity can be enhanced by doping with metallic elements such as Cr, V, Fe, and so on [12–14]. However, TiO<sub>2</sub> doped by a single element has not been found to meet practical requirements and co-doping with different elements may lead to better synergistic effects. Co-doped TiO<sub>2</sub> materials include S–N-co-doped TiO<sub>2</sub> [15], F–N-co-doped TiO<sub>2</sub> [16–19], B–N-co-doped TiO<sub>2</sub> [20], C–N-co-doped TiO<sub>2</sub> [21], La–F co-doped TiO<sub>2</sub> [22] and C–N–F co-doped TiO<sub>2</sub> powders [23]. Not only can the optical absorption efficiency be improved, but also the physical origin of the photocatalytic activity improvement has been clarified. For example, N–F co-doped TiO<sub>2</sub> has a smaller number of oxygen defects than the N-doped materials and

this is probably the reason for the better photostability and photocatalytic activity.

Co-doping does not, however, guarantee success and the proper choice of dopants is crucial. In this work, a series of TiO<sub>2</sub> samples co-doped with F and Fe were prepared through peroxidation at low temperature. The photocatalytic properties of the catalysts were determined by monitoring the degradation of methylene blue (ML) and the results show that compared to the undoped and singly-doped TiO<sub>2</sub>, the photocatalytic effect of the co-doped TiO<sub>2</sub> is the highest due to the synergistic effects rendered by dual element doping.

## 2 Experimental details

### 2.1 Materials

Titanium tetrachloride (TiCl<sub>4</sub>) is industrial grade and ammonia (NH<sub>3</sub>·H<sub>2</sub>O), ammonium fluoride (NH<sub>4</sub>F) and hydrogen peroxide (H<sub>2</sub>O<sub>2</sub>) are chemically pure. methylene blue (ML) was analytical and purchased from Beijing co., Ltd.

### 2.2 Preparation

The F-doped, Fe-doped and F–Fe-co-doped TiO<sub>2</sub> materials were prepared by a stepwise sol–gel reaction and hydrogen peroxide oxidation [24]. First of all, 0.3–0.6 mol/L titanium tetrachloride solutions were prepared and then appropriate amounts of the raw material containing the doping elements (NH<sub>4</sub>F or FeCl<sub>3</sub> or NH<sub>4</sub>F and FeCl<sub>3</sub>) were added to produce the solutions which had mass ratios of F<sup>−</sup> to Ti<sup>4+</sup>, Fe<sup>3+</sup> to Ti<sup>4+</sup>, and (F<sup>−</sup> + Fe<sup>3+</sup>) to Ti<sup>4+</sup> to be 0.15, 0.15 and 0.30%, respectively. The composition of the samples is summarized in Table 1. The system was kept for 24 h without stirring and then an ammonia solution was added slowly to obtain a pH value of 10. The precipitate formed was washed with distilled water 6 to 8 times to remove impurities. Subsequently, distilled water was used to dilute the slurry to yield a suspension (about 10 g of sediment in 0.1 L of water) and saturated hydrogen peroxide was dropped using a drip funnel until an orange-red transparent solution was formed. The solution was heated to 80–100 °C for 8 h to form the sol. The TiO<sub>2</sub> and doped TiO<sub>2</sub> were used or freeze dried to produce powders of TiO<sub>2</sub> and doped TiO<sub>2</sub> for further studies.

### 2.3 Characterization

X-ray diffraction (XRD) was performed on a D/max-rA 12kw diffractometer (Beijing) using the Cu K<sub>α</sub> ( $\lambda = 1.5406\text{\AA}$ ) radiation to determine the crystal structure

of the TiO<sub>2</sub> and doped TiO<sub>2</sub> powders. The UV–visible diffuse reflection spectra were acquired on a UV–visible spectrophotometer (UV-λ900LMADDA, USA) with a light path length of 1 cm. The morphology of the TiO<sub>2</sub> and doped TiO<sub>2</sub> sol was observed by a transmission electron microscope (TEM; JEM-100CX, JEOL) at an acceleration voltage of 200 kV.

The photocatalytic activity of the samples was evaluated by monitoring the degradation of ML. A 10 mg/L standard solution of ML was kept in the dark for about 12 h. While magnetically stirred, an appropriate amount of the catalyst was added to produce a suspension. The concentration of TiO<sub>2</sub> in the suspension was about 3 wt%. The suspension was irradiated with sun light (intensity of about 25 mW/cm<sup>2</sup>) for 4 h and then centrifuged at a speed of 3,000 r/min for 15 min to yield a clear solution. The concentration of methylene blue in the solution was determined by the spectrophotometry at 665 nm in order to evaluate the optical catalytic effect. The decolorization rate  $\eta$  was determined in accordance with the photocatalytic activity of TiO<sub>2</sub> as shown in the following:

$$\eta = (A - A_o)/A_o \times 100\%,$$

where  $A_o$  is the absorbance of initial methylene blue solution and  $A$  is the the absorbance of the methylene blue solution after photocatalytic degradation by TiO<sub>2</sub> and doped TiO<sub>2</sub>.

## 3 Results and discussion

### 3.1 XRD

Figure 1 shows the XRD patterns acquired from the pure TiO<sub>2</sub>, F-TiO<sub>2</sub>, Fe-TiO<sub>2</sub>, and F<sub>0.15</sub>-Fe<sub>0.15</sub> co-doped TiO<sub>2</sub>. The diffraction peak at 25.28° observed from the XRD pattern of the pure TiO<sub>2</sub> shows that the main crystal phase is anatase, and the peak at 27.4° indicates the presence of the rutile phase. All the peaks in the XRD patterns of the F and Fe singly-doped TiO<sub>2</sub> can be designated to the anatase phase (most active phase) without any indication of other crystalline phases such as rutile or dopant related ones. As a variant valence metal cation, Fe ions can react with Ti<sup>4+</sup> on the surface of TiO<sub>2</sub>, and Ti<sup>4+</sup> is reduced to Ti<sup>3+</sup> which inhibits the transformation of anatase to rutile [25]. Fluorine ions also enhance the crystallization of the anatase phase [26]. It leads to the reduction in the oxygen vacancies on the TiO<sub>2</sub> surface and suppresses the crystallization of other phases by adsorbing onto the surface of the TiO<sub>2</sub> particles [27]. Fe and F lead to the formation of Fe-TiO<sub>2</sub> and F-TiO<sub>2</sub> resulting in the formation of the complete anatase phase, but in the XRD pattern of F–Fe co-doped TiO<sub>2</sub>, the (110) diffraction peak at 27.4 ° of the rutile phase

**Table 1** Composition and adsorption edge of  $\text{TiO}_2$  powders

Samples	Composition	Adsorption edge (nm)	Degradation of ML (%)
Pure $\text{TiO}_2$	$\text{TiO}_2$	386	43
F- $\text{TiO}_2$	$\text{F}^-/\text{Ti}^{4+}=0.15 \text{ mol\%}$	420	60
Fe- $\text{TiO}_2$	$\text{Fe}^{3+}/\text{Ti}^{4+}=0.15 \text{ mol\%}$	478	68
$\text{F}_{0.15}\text{-Fe}_{0.15}\text{-TiO}_2$	$\text{F}^-/\text{Ti}^{4+}=0.15 \text{ mol\%}$ , $\text{Fe}^{3+}/\text{Ti}^{4+}=0.15 \text{ mol\%}$	510	76
$\text{F}_{0.10}\text{-Fe}_{0.20}\text{-TiO}_2$	$\text{F}^-/\text{Ti}^{4+}=0.10 \text{ mol\%}$ , $\text{Fe}^{3+}/\text{Ti}^{4+}=0.20 \text{ mol\%}$	—	70
$\text{F}_{0.20}\text{-Fe}_{0.10}\text{-TiO}_2$	$\text{F}^-/\text{Ti}^{4+}=0.20 \text{ mol\%}$ , $\text{Fe}^{3+}/\text{Ti}^{4+}=0.10 \text{ mol\%}$	—	65

is detected again. It may be because the Fe–F co-doped  $\text{TiO}_2$  reduces the effects of phase transformation inhibition and the rutile phase observed from the Fe–F co-doped  $\text{TiO}_2$ .

The average unit dimension of anatase in all of the samples is almost unchanged. Incorporation of F does not give rise to a significant change in the average unit cell dimension since the bond lengths of Ti–F (2.022 and 2.253 Å) are similar to those of Ti–O bonds (1.940 and 2.000 Å), even though a F atom has a smaller radius (0.57 Å) than oxygen atom (0.60 Å) [28].  $\text{Fe}^{3+}$  (0.64 Å) has a similar radius as  $\text{Ti}^{4+}$  (0.62 Å) and can penetrate easily into the crystal lattice of the  $\text{TiO}_2$  [29]. The small doping concentration may also be reason for the insignificant changes in the crystalline structure.

The XRD patterns show that all of the peaks are widened. It may be because the crystalline degree of  $\text{TiO}_2$  is not very high or the long-term order has been destroyed since the particle size is in nanometer region as determined by TEM.

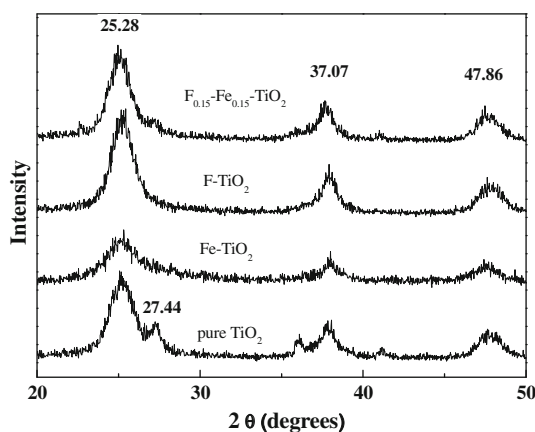
### 3.2 TEM

The morphology of the pure  $\text{TiO}_2$  sol and doped  $\text{TiO}_2$  sols diluted by distilled water to the detection limit of TEM is depicted in Fig. 2. The particle size of the singly doped  $\text{TiO}_2$  is about a few nanometer and decreases compared to pure  $\text{TiO}_2$  (50–70 nm). In comparison, the co-doped  $\text{TiO}_2$  has almost the same diameter as pure  $\text{TiO}_2$ . The results indicate that the single doping by F or Fe can influence the condensation reaction of hydroxide in the presence of hydrogen peroxide and inhibit the particle size growth. Meanwhile, since the doping reaction takes place in the solution in which the reaction can proceed more easily than in a solid reaction, the presence of fluorine or Fe has a significant effect on the particle morphology. However, the combined effect of F and Fe diminishes the influence of F or Fe on the particle size. These results and the XRD data show that co-doping with Fe and F has no obvious influence on the particle size and crystalline structure compared to doping by Fe or F. In the TEM micrographs, agglomeration is observed due to the high surface energy of  $\text{TiO}_2$  [23].

### 3.3 UV–visible diffuse reflectance spectra

The light absorption characteristics of  $\text{TiO}_2$  is changed after doping and the UV–vis diffuse reflectance spectra are usually used to investigate the band structure of  $\text{TiO}_2$  [30]. As shown in Fig. 3, compared to pure  $\text{TiO}_2$ , the absorption spectra of the doped  $\text{TiO}_2$  expand into the visible region. The adsorption edge and red shifts are summarized in Table 1.

The absorption edge of the F doped  $\text{TiO}_2$  does not display an appreciable shift to the visible region, indicating that F doping does not cause an absorption edge red shift which is consistent with the report by Huaming Yang [24]. When the concentration of Fe is 0.15%, the adsorption edge of the Fe- $\text{TiO}_2$  red shifts to about 478 nm. With F and Fe co-doping, further red shift can be observed from the

**Fig. 1** XRD patterns of doped  $\text{TiO}_2$

**Fig. 2** TEM images of pure  $\text{TiO}_2$  and doped  $\text{TiO}_2$ : **a** pure  $\text{TiO}_2$ , **b** Fe- $\text{TiO}_2$ , **c** F- $\text{TiO}_2$ , and **d**  $\text{F}_{0.15}\text{-Fe}_{0.15}\text{-TiO}_2$

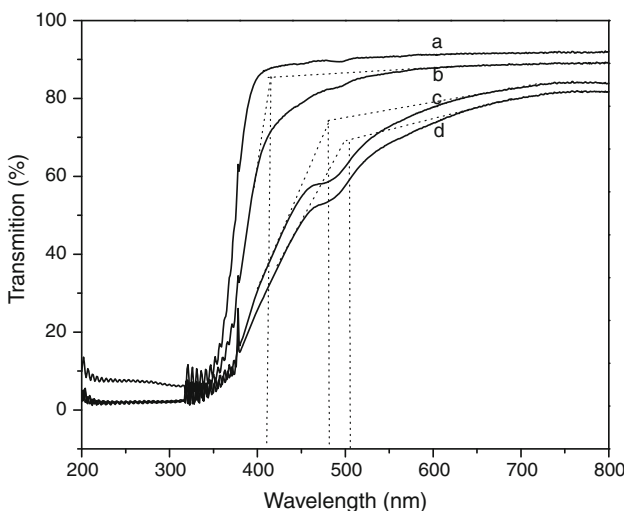
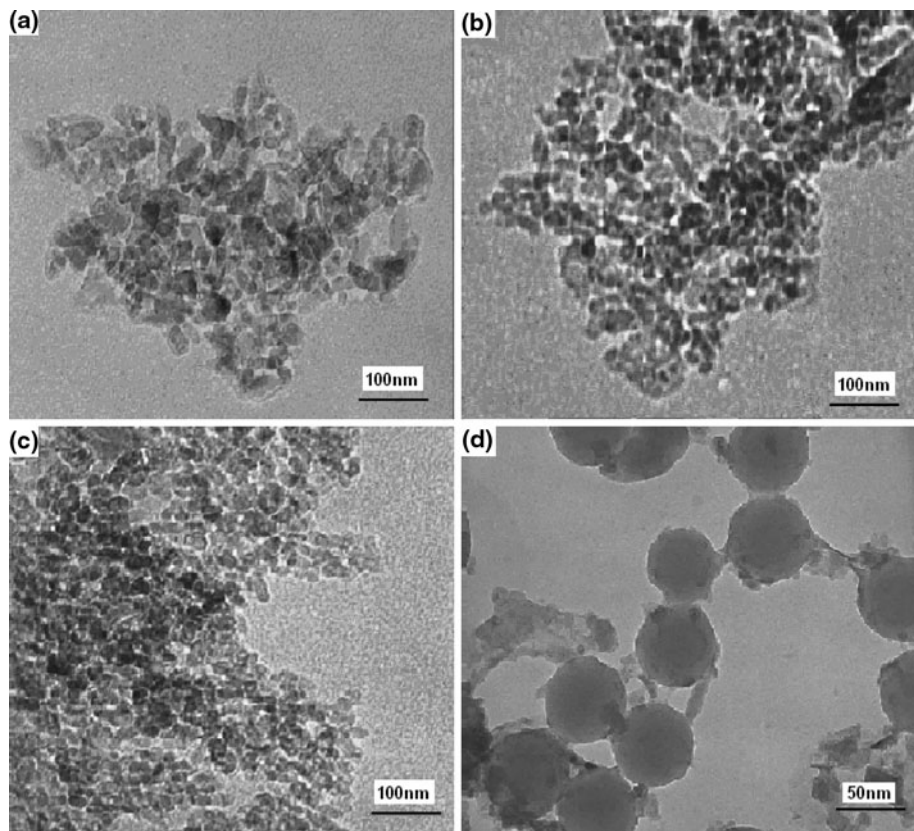


**Fig. 3** UV-visible diffuse reflectance spectra of  $\text{TiO}_2$  powders: **a** pure  $\text{TiO}_2$ , **b** F- $\text{TiO}_2$ , **c** Fe- $\text{TiO}_2$ , **d**  $\text{F}_{0.15}\text{-Fe}_{0.15}\text{-TiO}_2$

spectra. According to quantum effect, the absorption edge should blue shift with the particle size, but co-doping with F and Fe results in a red shift in the adsorption edge [31]. The UV-vis diffuse reflectance data show that the influence of Fe on the adsorption edge shift is larger than that rendered by F. As a result of the combined effects of F and Fe, the adsorption edge of the co-doped  $\text{TiO}_2$  shifts from

386 nm to 510 nm and the co-doped  $\text{TiO}_2$  shows the largest magnitude.

### 3.4 Photocatalytic properties

Figure 4 shows the photocatalytic degradation of MB in the presence of the pure  $\text{TiO}_2$ , F- $\text{TiO}_2$ , Fe- $\text{TiO}_2$ , and F-Fe co-doped  $\text{TiO}_2$  samples. After irradiating with visible light for 4 h, the degradation rate of MB catalyzed by pure  $\text{TiO}_2$  is about 43%, whereas that catalyzed by  $\text{TiO}_2$  doped by Fe or F increases to 68 and 60%, respectively. The enhanced photocatalytic activity of the F-doped  $\text{TiO}_2$  can be mainly attributed to the larger area on the active site of the  $\text{TiO}_2$  [24]. The enhanced photocatalytic activity results from the crystal distortion when  $\text{Fe}^{3+}$  partly substitutes for  $\text{Ti}^{4+}$  in the  $\text{TiO}_2$  lattice, and the absorption edge of  $\text{TiO}_2$  red shifts to a longer wavelength. Hence, more carriers are generated under visible light irradiation thereby increasing the photocatalytic efficiency [14]. A 76% degradation rate, the highest of all samples, is observed from the F-Fe co-doped- $\text{TiO}_2$ . The phenomena can be attributed to the incorporation of metal ions which not only inhibit complexing of the non-metallic photo-carriers but also improve the mutual effects of the photocatalytic properties.

When the content of F and Fe in the system is constant, a decreased degradation rate is observed with different ratios

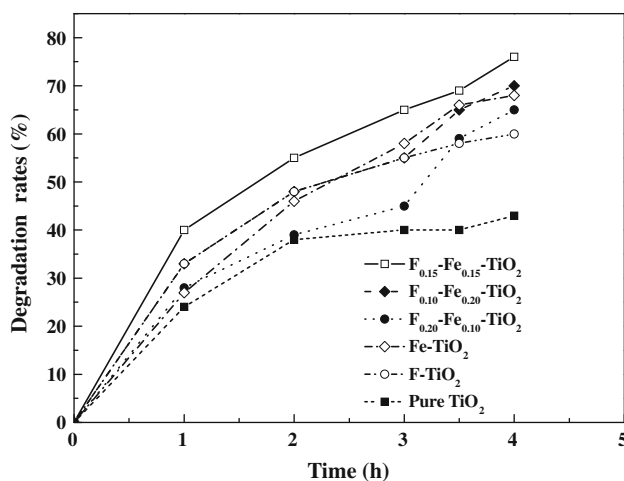


**Fig. 4** Photoactivity of TiO<sub>2</sub> sols

of F to Fe. Fe as an electron donor plays an important role in the doped materials. With increasing Fe concentration, the absorption edge of the TiO<sub>2</sub> red shifts to a longer wavelength and more TiO<sub>2</sub> are thus active under visible light irradiation naturally enhancing the photocatalytic efficiency [32]. However, Fe may also act as the recombination centers for the photogenerated carriers and so the Fe exceeds a certain concentration (0.15%), the photocatalytic efficacy is reduced. Based on our experiments, the best doping ratio is F:Fe:Ti = 0.15:0.15:100.

#### 4 Conclusion

F–Fe co-doped TiO<sub>2</sub> sols are prepared by peroxidation using FeCl<sub>4</sub> and NH<sub>4</sub>F as the doping materials at low temperature. The structure, morphology, light adsorption, and catalytic efficiency (monitored by ML degradation) are determined. The results show that the crystal structure of F–Fe co-doped TiO<sub>2</sub> contains both the anatase and rutile phases and are different to the phases observed from singly-doped TiO<sub>2</sub>. F or Fe doping inhibits size growth of TiO<sub>2</sub> but this phenomenon is not observed from the co-doped TiO<sub>2</sub>. The photocatalytic efficiency of the F–Fe co-doped TiO<sub>2</sub> increases to 76% (the highest of all samples) since the light adsorption edge red shifts to 510 nm. The best doping ratio is found to be F:Fe:Ti = 0.15:0.15:100.

**Acknowledgments** This research was financially supported by Key Project of Chinese Ministry of Education (No:107023), the special co-construction project of Beijing city education committee, City University of Hong Kong Strategic Research Grant (SRG) No. 7008009, and Doctoral Program Foundation of Institution of higher education of China(2-2-08-07).

#### References

1. Fujishima A, Honda K (1972) Nature 238:37
2. Maldotti A, Molinari A, Amadelli R (2002) Chem Rev 102:3811
3. Hoffmann MR, Martin ST, Choi W (1995) Chem Rev 95:69
4. Linsebigler AL, Lu G, Yates JT (1995) Chem Rev 95:735
5. Nonami T, Hase H, Funakoshi K (2004) Catal Today 96:113
6. Yanagida S, Senadeera GKR, Nakamura K (2004) J Photochem Photobiol A Chem 166(1–3):75
7. Senadeera GKR, Kitamura T, Wada Y (2004) J Photochem Photobiol A Chem 164(1–3):61
8. Asahi RT, Morikawa T, TOhwaki, K Aoki, Taga Y (2001) Science 293:269
9. Khan SUM, Al-Shahry M, Ingler WB (2002) Science 297:2243
10. Yu JC, Yu J, Ho W, Jiang Z, Zhang L (2002) Chem Mater 14:3808
11. Pore V, Ritala M, Leskela M, Areva S, Jarn M, Jarnstrom J (2007) J Mater Chem 17:1361
12. Dvoranova D, Brezova V, Mazur M, Malati MA (2002) Appl Catal B Environ 37:91
13. Martin ST, Morrison CL, Hoffmann MR (1994) J Phys Chem 98:13695
14. Cui LF, Wang YS, Niu MT, Chen GX, Cheng Y (2009) J Solid State Chem 182:2785
15. Xu JH, Li J, Dai WL, Cao Y, Li H, Fan K (2008) Appl Catal B Environ 79:72
16. Li D, Haneda H, Hishita S, Ohashi N (2005) Chem Mater 17:2588
17. Li D, Ohashi N, Hishita S, Kolodiaznyi T, Haneda H (2005) J Solid State Chem 178:3293
18. Huang DG, Liao SJ, Liu JM, Dang Z, Petrik L (2006) J Photochem Photobiol A Chem 184:282
19. Valentin CD, Finazzi E, Pacchioni G (2008) Chem Mater 20:3706
20. Liu G, Zhao Y, Sun C, Li F, Lu GQ, Cheng HM (2008) Angew Chem Int Ed 47:4516
21. Yang X, Cao C, Erickson L, Hohn K, Maghirang R, Klabunde K (2008) J Catal 260:128
22. Cao GX, Li YG, Zhang QH, Wang HZ (2010) J Am Ceram Soc 93:1252
23. Xu QC, Wellia DV, Sk MA, Lim KH, Loo JSC, Liao DW, Amal R, Tan TTY (2010) J Photochem Photobio A Chem 210:181
24. Yang HM, Zhang XC (2009) J Mater Chem 19:6907
25. Mackenzie KJD (1975) Trans J Br Ceram Soc 74:29
26. Yu JG, Yu JC, Cheng B, Hark SK, Iu K (2003) J Solid State Chem 174:372
27. Yu JG, Yu JC, Ho WK, Jiang ZT, Zhang LZ (2002) Chem Mater 14:3808
28. Pelaez M, Cruz AA, Stathatos E, Falaras P, Dionysiou DD (2009) Catal Today 144:19
29. Yuan ZF, Zhang JL, Li B, Li JQ (2007) Thin Solid Films 515:7091
30. Ren WJ, Ai ZH, Jia FL, Zhang LZ, Fan XX, Zou ZG (2007) Appl Catal B Environ 69:138
31. Zhong M, Wei ZH, Si PZ, Li H, Wei GY, Ge HL, Han GR (2010) J Chin Ceram Soc 38:68
32. Choi W, Termin A, Hoffmann MR (1994) J Phys Chem 98:13669